

Lithium insertion and extraction kinetics of $\text{Li}_{1+x}\text{V}_3\text{O}_8$

Jin Kawakita^{*}, Takashi Miura, Tomiya Kishi

Department of Applied Chemistry, Faculty of Science and Technology, Keio University, Hiyoshi 3-14-1, Kouhoku-ku, Yokohama 223-8522, Japan

Received 12 February 1999; accepted 30 March 1999

Abstract

Lithium insertion and extraction kinetics of lithium trivanadate, $\text{Li}_{1+x}\text{V}_3\text{O}_8$, was investigated by using the electrochemical measurements at various temperatures and current densities. The results showed that the reaction rates of both insertion and extraction were limited by the small diffusivity of Li^+ ions in the $\text{Li}_4\text{V}_3\text{O}_8$ phase formed for $x > 1.5$ upon lithiation. Extraction reaction was also dependent on the thermodynamic factor on the basis of the incomplete reversibility of transformation from the $\text{Li}_4\text{V}_3\text{O}_8$ phase to the original LiV_3O_8 one. © 1999 Elsevier Science S.A. All rights reserved.

Keywords: Vanadate; Lithium; Insertion; Extraction; Kinetics

1. Introduction

Some vanadium oxides such as V_2O_5 and V_6O_{13} have been investigated as cathode materials for secondary lithium batteries [1]. These vanadates possess relatively larger practical discharge capacities as compared with other transition metals, e.g., LiCoO_2 . In both vanadates, however, the large-capacity retentivity is incompatible with the high-rate capability in repeated discharge and charge cycles. A multidimensional structure restrained the modification of the host-lattice during lithium intercalation and deintercalation of the guest species, i.e., lithium, leading to a lowering of the capacity loss. Simultaneously, the reaction rates of intercalation and deintercalation become smaller owing to a decrease in the number of the diffusion path of lithium. Lithium trivanadate, $\text{Li}_{1+x}\text{V}_3\text{O}_8$ is a promising alternative to these vanadates [2–4]. This oxide has a layered structure where pre-existing Li^+ ions at octahedral sites attach adjacent layers strongly [5]. Over three equivalents of Li^+ ions can be inserted/extracted in LiV_3O_8 reversibly because of both the outstanding structural stability and empty sites for Li^+ ion occupation between the layers [6]. Furthermore, Li^+ ions at octahedral

sites are no hindrance to jumping of Li^+ ion from one tetrahedral site to other [7], and the diffusion of lithium in LiV_3O_8 is faster than those in V_2O_5 and V_6O_{13} [1]. Much effort has been made to improve the electrochemical performance of LiV_3O_8 . These were adaptation of the samples with different degrees of crystallinity [2,8–11], modification of the host framework [2,12,13], introduction of alien atoms and molecules between the layers [2,14–16], and fabrication of the electrode with the small particle size and the large contact area between components [2,11,17,18].

The crystal structure of LiV_3O_8 was refined by using X-ray diffractometry (XRD) [5,19,20]. Other properties were analyzed by infrared (IR) [20,21] and Raman spectroscopy [20], and ^7Li nuclear magnetic resonance (NMR) [22]. Lithium insertion behaviour of LiV_3O_8 was reported in terms of the crystal structure and thermodynamics. Changes of the atomic arrangement and the coordination state of the vanadium atom upon lithiation were characterized by XRD [6,7,19,23–25], IR [20,25,26], Raman [20], and X-ray absorption spectroscopic (XAS) [26] measurements. The thermodynamic data such as enthalpy (ΔH), entropy (ΔS) of lithiation, and the site energy of inserted lithium were estimated by using solution calorimetry [3], coulometric titration [23,27], and theoretical calculation [28]. From these results, lithium insertion reaction of $\text{Li}_{1+x}\text{V}_3\text{O}_8$ is summarized as follows. It is described as three steps composed of a single-phase reaction for the range $0 < x < 2.0$ in $\text{Li}_{1+x}\text{V}_3\text{O}_8$, a two-phase reaction for $2.0 < x < 3.2$, and a single-phase reaction for $3.2 < x < 4.0$.

^{*} Corresponding author. Tel.: +81-45-563-1141; Fax: +81-45-563-5967; E-mail: kawakita@chem.keio.ac.jp

Phase transformation occurs at $x = 2.0$ from the original LiV_3O_8 phase to the second $\text{Li}_4\text{V}_3\text{O}_8$ one. Some authors [25,27,29] reported that the first single phase ends a bit earlier at a composition $\text{Li}_{2.5}\text{V}_3\text{O}_8$ ($x = 1.5$). Although lithium extraction is a reversible reaction, the delithiated material has a slightly modified structure, as compared with original LiV_3O_8 [19,30].

Most of works on lithium insertion behaviour of LiV_3O_8 have been discussed from the standpoint of equilibrium, as mentioned above. The actual reaction, however, depends considerably also on the kinetic factors controlled by the current density. The diffusion coefficient of lithium was measured at various x values during lithiation [7,17,23,26], and yet its contribution to the reaction rate in each depth of discharge was not elucidated. In this paper, lithium insertion and extraction reactions were characterized in a dynamic state by using electrochemical measurements varying temperature and current density.

2. Experimental

The lithium trivanadate, LiV_3O_8 , was prepared by the high temperature synthesis of Li_2CO_3 and V_2O_5 as described elsewhere [13]. The chemical analysis of the obtained compound results in the nominal composition, $\text{Li}_{1.2}\text{V}_3\text{O}_8$. All ground powder samples were sieved under $38 \mu\text{m}$ in particle size.

Electrochemical measurement was carried out using a cylindrical glass with three electrodes filled with argon gas. All the procedures for this experiment were presented elsewhere in detail [24]. The working electrode was a pressed pellet composed of a mixture of powder sample of LiV_3O_8 , acetylene black and PTFE in a weight ratio of 80:15:5. The counter- and reference electrodes were lithium metal rods. The electrolyte was $1 \text{ mol dm}^{-3} \text{ LiClO}_4/\text{PC}$ solution. The cell was set into a thermostatic water bath at a temperature of 5° , 25° or 45°C . To protect a separation of two parts caused by expansion of the internal gas and by rising of the vapor pressure of the electrolyte solvent with increase in the temperature of the cell, pulling the gas out reduced the internal pressure of the cell to some extent. In addition, the upper part of the cell was attached tightly with the lower one. Galvanostatic discharge and discharge/charge tests were performed at current densities of ± 100 , 200, 500 and $1000 \mu\text{A cm}^{-2}$ with a galvanostat controlled by a personal computer. The potential limits were 1.5 and 3.6 V vs. Li/Li^+ on discharge and charge processes, respectively. The chemical diffusion coefficient of lithium, \tilde{D}_{Li} , was determined by the galvanostatic intermittent titration technique (GITT) [31]. In this paper, discharge and charge capacities are represented by x and y , respectively, corresponding to the values per formula unit calculated from the amount of electricity passed through the working electrode during discharge and charge.

3. Results and discussion

3.1. Insertion kinetics

Fig. 1 shows a dependence of the discharge capacity (x) of LiV_3O_8 on the current density at 5° , 25° and 45°C . Naturally, a larger capacity is attained at a smaller current density and at a higher temperature. In the current density of 100 to $1000 \mu\text{A cm}^{-2}$, the maximum capacity loss is 40%. Furthermore, when the temperature varies from 45° to 5°C , the capacity decreases by about 35% at each current density. These results indicate that overall lithium insertion reaction of LiV_3O_8 is considerably affected by the kinetic factor, the effect of which does not appear clearly on each step of the reaction.

On the discharge curve, the features such as inflexion and hump became rapidly obscure with increase in the current density from 100 to $1000 \mu\text{A cm}^{-2}$ even at 45°C . Fig. 2 shows discharge curves of LiV_3O_8 at $-100 \mu\text{A cm}^{-2}$ at constant temperatures of 5° , 25° and 45°C . Effects of temperature on the shape of the discharge curve divide all the curves into two regions near $x = 1.5$ and an arrow represents the dividing point. Note that x value contains excess 0.2 equivalent of Li^+ ion in preparation. Up to about $x = 1.5$ [region 1 (Δx_1): composed of the first to the third step], the shape seems almost independent of temperature. In contrast, temperature effect is remarkable for $x > 1.5$ [region 2 (Δx_2): composed of the fourth and further steps up to 2.0 V]. It was reported that the open circuit potential (OCP) was almost independent of temperature while the gaps between OCP and discharge potential were larger in the second region [24]. Accordingly, the kinetic factors of lithium insertion process appear in the second region.

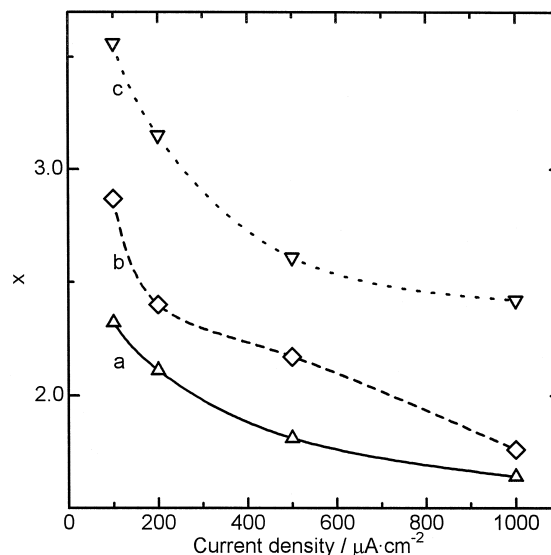


Fig. 1. Dependence of discharge capacity (x) on current density at (a) 5° , (b) 25° , and (c) 45°C .

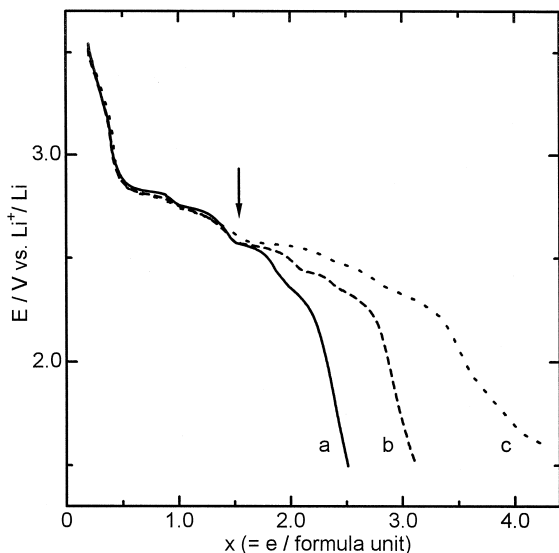


Fig. 2. Discharge curves of LiV_3O_8 at $-100 \mu\text{A cm}^{-2}$ at (a) 5° , (b) 25° , and (c) 45°C .

These temperature effects can also clearly be seen by plotting the extent of lithium insertion (Δx) of each region, as shown in Fig. 3. Regardless of both temperature and current density, Δx_1 keeps an almost constant value of about 1.5. This might be caused by sufficiently fast diffusion of Li^+ ions in the original LiV_3O_8 phase under this experimental condition. On the other hand, Δx_2 depends on the temperature and on the current density. In this region, formation of the $\text{Li}_4\text{V}_3\text{O}_8$ phase is considered to reduce an overall diffusivity of lithium, even in the coexistence state of both the original LiV_3O_8 and the second $\text{Li}_4\text{V}_3\text{O}_8$ phases.

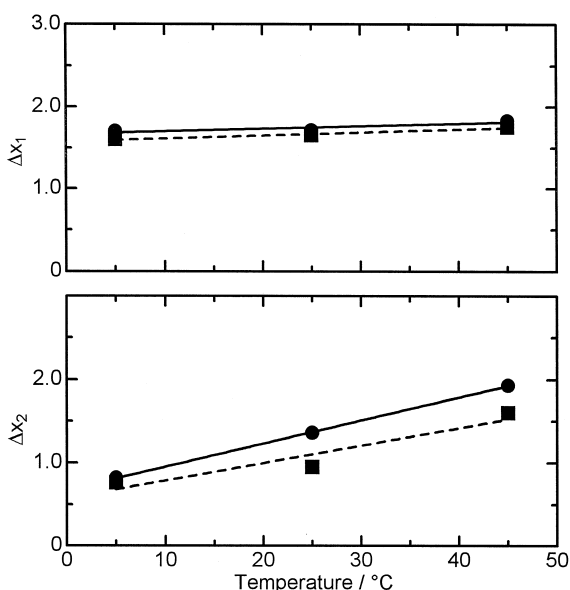


Fig. 3. Dependence of extent of lithium insertion (Δx) on temperature, (cd \bullet : -100 and \blacksquare : $-200 \mu\text{A cm}^{-2}$).

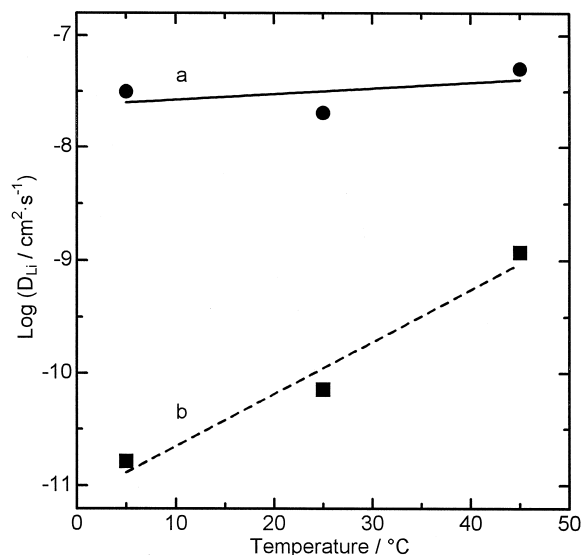


Fig. 4. Dependence of chemical diffusion coefficient of lithium, on temperature in (a) LiV_3O_8 phase at $x = 0.2$ and (b) $\text{Li}_4\text{V}_3\text{O}_8$ phase at $x = 3.6$.

With respect to apparent chemical diffusion coefficient (\bar{D}_{Li}), the $\text{Li}_4\text{V}_3\text{O}_8$ phase is compared with the LiV_3O_8 one at various temperatures, as shown in Fig. 4. Note that diffusion coefficients in two phases correspond to the values for the starting and the lithiated materials with nominal compositions of $\text{Li}_{1.2}\text{V}_3\text{O}_8$ ($x = 0.2$) and $\text{Li}_{4.6}\text{V}_3\text{O}_8$ ($x = 3.6$), respectively. Apparently, the diffusion coefficient in the $\text{Li}_4\text{V}_3\text{O}_8$ phase increases gradually from 10^{-11} to $10^{-9} \text{ cm}^2 \text{ s}^{-1}$ with increase in the temperature, as compared with nearly constant values at the order of $10^{-8} \text{ cm}^2 \text{ s}^{-1}$ in the LiV_3O_8 phase.

These results reveal that the dependence of Δx_2 on some kinetic parameters is due to a small diffusivity of Li^+ ions in the second $\text{Li}_4\text{V}_3\text{O}_8$ phase, which is formed beyond $x = 1.5$ and coexists together with the original LiV_3O_8 phase. In addition, a much smaller diffusivity of Li^+ ions in the $\text{Li}_4\text{V}_3\text{O}_8$ phase might cause a retardation of further insertion of lithium beyond $x = 1.5$, where lithium insertion into the LiV_3O_8 phase as the single-phase reaction changes to insertion into the $\text{Li}_4\text{V}_3\text{O}_8$ phase formed on the LiV_3O_8 phase.

3.2. Extraction kinetics

Fig. 5 shows a dependence of the charge capacity (y) of LiV_3O_8 on the current density at 5° , 25° and 45°C . Similarly to the case of discharge process, the charge capacity becomes larger at a smaller current density. This profile, however, does not express an accurate effect of the extraction kinetics on the reaction because of non-identical condition of the lithiated compounds before charging with respect to the crystal structure and the lithium content.

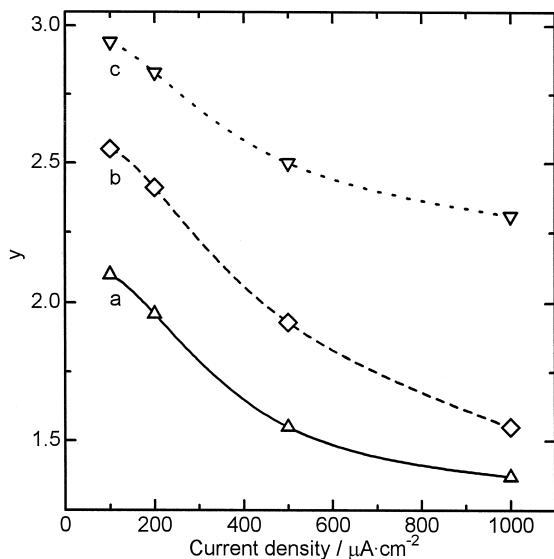


Fig. 5. Dependence of charge capacity (y) on current density at (a) 5°, (b) 25°, and (c) 45°C.

On the charge curves of LiV_3O_8 at $+100 \mu\text{A cm}^{-2}$ at 5°, 25° and 45°C, some steps are observed and in particular, obviously at 45°C (as shown in Fig. 6). Effects of temperature on the shape of the charge curve divide all the curves into three regions and two arrows represent the dividing points. These regions are in turn termed as Δy_1 , Δy_2 and Δy_3 with increase in the y value. During charge of $\text{Li}_{1+x}\text{V}_3\text{O}_8$ with a high lithium content, it was reported that disappearance of the $\text{Li}_4\text{V}_3\text{O}_8$ phase and simultaneous formation of the LiV_3O_8 phase occur in the early stage of lithium extraction reaction, and followed by a delithiation process in the single LiV_3O_8 phase [30]. Therefore, lithium extraction reaction is supposed to proceed in the region of Δy_1 where the $\text{Li}_4\text{V}_3\text{O}_8$ phase might exist, and succes-

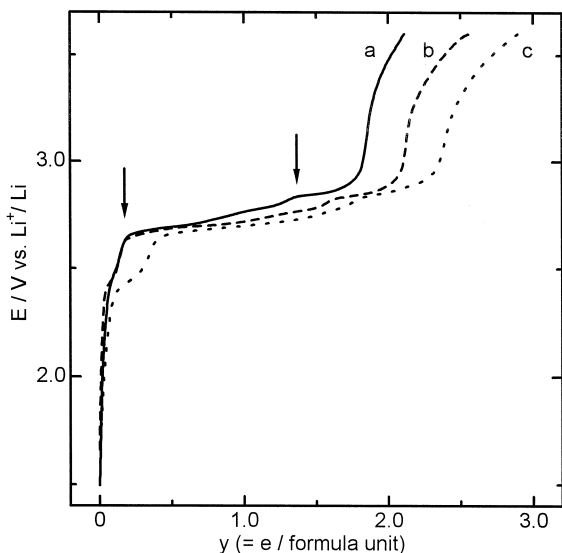


Fig. 6. Charging curves of LiV_3O_8 at $+100 \mu\text{A cm}^{-2}$ at (a) 5°, (b) 25° and (c) 45°C.

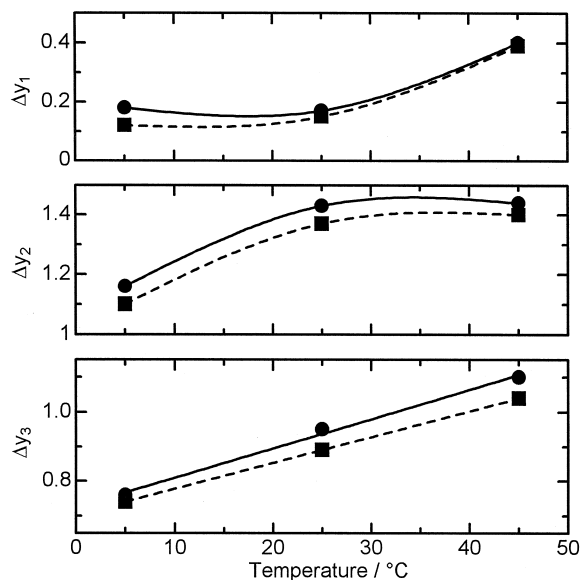


Fig. 7. Dependence of extent of lithium extraction (Δy) on temperature, (cd) ●: $+100$ and ■: $+200 \mu\text{A cm}^{-2}$.

sively in two regions of Δy_2 and Δy_3 where reactions occur in different mechanisms.

The features such as inflexion and hump became rapidly obscure also on the charge curve with increase in the current density. Then, temperature dependence of the extent of lithium extraction (Δy) in each region is compared in Fig. 7. In the first region, Δy_1 is less than 0.2 at both 5° and 25°C, and yet it increases to about 0.4 at 45°C. This result indicates occurrence of lithium extraction from the $\text{Li}_4\text{V}_3\text{O}_8$ phase in this region. When the amount of inserted lithium (x) exceeds 3.0 during discharge, additional lithium is certainly accommodated in the $\text{Li}_4\text{V}_3\text{O}_8$ phase, and might be extracted in the early stage of the charge process.

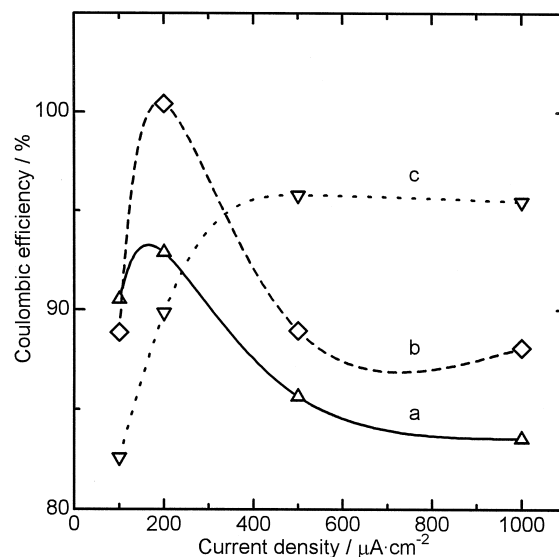


Fig. 8. Dependence of coulombic efficiency on current density at (a) 5°, (b) 25°, and (c) 45°C.

In the second region, Δy_2 increases and does not surpass 1.5 with increase in the temperature. This phenomenon indicates a presence of the extraction limit in this region where the reproduced LiV_3O_8 phase exists. In the third region, a linear increase in Δy_3 is observed as the temperature rises. Temperature dependence is observed clearly in the last stage of the charge process. It was reported that the structure of slightly lithiated compound, $\text{Li}_{1+x}\text{V}_3\text{O}_8$ ($x < 0.5$), is a less distorted configuration, as compared with the 'non'-lithiated one, LiV_3O_8 [19,30]. Accordingly, lithium needs to be extracted from more stable tetrahedral sites in the region (Δy_3) with a small x value. Taking into account the sufficiently fast diffusion of lithium in the LiV_3O_8 phase, temperature dependence of Δy_3 is explained in terms of equilibrium rather than kinetics. Increase in temperature makes delithiated LiV_3O_8 possible to exist in a less stable state with the more distorted configuration. In addition, equilibrium is shifted to the direction of extraction of lithium because lithium insertion reaction of $\text{Li}_{1+x}\text{V}_3\text{O}_8$ is exothermic [3].

Dependence of the coulombic efficiency on the current density in the first cycle at 5°, 25° and 45°C is shown in Fig. 8. It is equal to the capacity ratio of charge vs. discharge. At 100 $\mu\text{A cm}^{-2}$, the efficiency becomes smaller with increase in the temperature. This phenomenon is caused by rearrangement of the host lattice accompanying the phase transformation and by incomplete reversibility of rearrangement during lithium insertion and extraction reactions. This hypothesis is supported by the report that the delithiated product is a slight modification of the parent structure, as described above. Though the current density increases from 100 to 200 $\mu\text{A cm}^{-2}$, the efficiency becomes larger. This is explained by the reason that in this current range, the discharge capacity has a larger decreasing rate than the charge capacity because of a larger decrement in the range for existence of the $\text{Li}_4\text{V}_3\text{O}_8$ phase with small diffusivity of lithium in the insertion process.

The slow diffusion of lithium in the $\text{Li}_4\text{V}_3\text{O}_8$ phase is responsible for determining of the reaction rate in the early stage of delithiation process. Under this experimental condition, there is no obvious effect of extraction kinetics on other regions. In the last stage, remaining lithium has difficulty in being extracted, owing to occupation of thermodynamically stable sites.

4. Conclusion

The discharge and charge behaviours depended remarkably on the temperature as well as the current density. Lithium insertion kinetics of $\text{Li}_{1+x}\text{V}_3\text{O}_8$ was affected largely by the small diffusivity of Li^+ ions in $\text{Li}_4\text{V}_3\text{O}_8$

phase formed for $x > 1.5$ upon lithiation. The similar result was found during lithium extraction process in the $\text{Li}_4\text{V}_3\text{O}_8$ phase.

The incomplete reversibility of phase transformation between the $\text{Li}_4\text{V}_3\text{O}_8$ and the LiV_3O_8 phases caused a decrease in the charge capacity, leading to a capacity loss during cycling.

References

- [1] J. Desilvestro, O. Haas, *J. Electrochem. Soc.* 137 (1990) 5C.
- [2] M. Pasquali, G. Pistoia, M. Tocci, V. Manev, R.V. Moshtev, *J. Electrochem. Soc.* 133 (1986) 2454.
- [3] G. Pistoia, F. Rodante, M. Tocci, *Solid State Ionics* 20 (1986) 25.
- [4] K. West, B. Zachau-Christiansen, M.J.L. Østergård, T. Jacobsen, *J. Power Sources* 20 (1987) 165.
- [5] A.D. Wadsley, *Acta Cryst.* 10 (1957) 261.
- [6] G. Pistoia, M. Pasquali, M. Tocci, R.V. Moshtev, V. Manev, *J. Electrochem. Soc.* 132 (1985) 281.
- [7] G. Pistoia, S. Panero, M. Tocci, R.V. Moshtev, V. Manev, *Solid State Ionics* 13 (1984) 311.
- [8] K. Nassau, D.W. Murphy, *J. Non-Cryst. Solids* 44 (1981) 297.
- [9] G. Pistoia, M. Pasquali, G. Wang, L. Li, *J. Electrochem. Soc.* 137 (1990) 2365.
- [10] K. West, B. Zachau-Christiansen, S. Skaarup, Y. Saidi, J. Barker, I.I. Olsen, R. Pynenburg, R. Koksang, *J. Electrochem. Soc.* 143 (1996) 820.
- [11] N. Kumagai, A. Yu, *J. Electrochem. Soc.* 144 (1997) 830.
- [12] J. Kawakita, M. Majima, T. Miura, T. Kishi, *J. Power Sources* 66 (1997) 135.
- [13] J. Kawakita, H. Katagiri, T. Miura, T. Kishi, *J. Power Sources* 68 (1997) 680.
- [14] V. Manev, A. Momchilov, A. Nassalevska, G. Pistoia, M. Pasquali, *J. Power Sources* 54 (1995) 501.
- [15] G. Pistoia, G. Wang, D. Zane, *Solid State Ionics* 76 (1995) 285.
- [16] J. Kawakita, K. Makino, Y. Katayama, T. Miura, T. Kishi, *Solid State Ionics* 99 (1997) 165.
- [17] G. Pistoia, M. Pasquali, M. Tocci, V. Manev, R.V. Moshtev, *J. Power Sources* 15 (1985) 13.
- [18] G. Pistoia, M. Pasquali, Y. Geronov, V. Manev, R.V. Moshtev, *J. Power Sources* 27 (1989) 35.
- [19] L.A. de Picciotto, K.T. Adendorff, D.C. Liles, M.M. Thackeray, *Solid State Ionics* 62 (1993) 297.
- [20] X. Zhang, R. Frech, *Electrochim. Acta* 43 (1998) 861.
- [21] Y. Kera, *J. Solid State Chem.* 51 (1984) 205.
- [22] T.K. Halstead, W.U. Benesh, R.D. Gulliver II, R.A. Huggins, *J. Chem. Phys.* 58 (1973) 3530.
- [23] G. Pistoia, M.L. Di Vona, P. Tagliatesta, *Solid State Ionics* 24 (1987) 103.
- [24] J. Kawakita, Y. Katayama, T. Miura, T. Kishi, *Solid State Ionics* 107 (1998) 145.
- [25] J. Kawakita, T. Miura, T. Kishi, *Solid State Ionics*, in press.
- [26] R. Tossici, R. Marassi, M. Berrettoni, S. Stizza, G. Pistoia, *Solid State Ionics* 57 (1992) 227.
- [27] I.D. Raistrick, *Rev. Chim. Miner.* 21 (1984) 456.
- [28] R. Benedek, M.M. Thackeray, L.H. Yang, *Phys. Rev. B* 56 (1997) 10707.
- [29] A. Hammou, A. Hammouche, *Electrochim. Acta* 33 (1988) 1719.
- [30] J. Kawakita, T. Miura, T. Kishi, *Solid State Ionics* 118 (1999) 141.
- [31] W. Weppner, R.A. Huggins, *J. Electrochem. Soc.* 124 (1977) 1569.